LARGE EDDY SIMULATIONS OF FLOW AROUND A CIRCULAR CYLINDER IN THE VICINITY OF A WALL AT REYNOLDS NUMBER OF 13100

Mia Abrahamsen Prsic [1], Muk Chen Ong [2], Bjørnar Pettersen [1], Dag Myrhaug [1]
[1] *Department of Marine Technology, Norwegian University of Science and Technology, NO-7491 Trondheim, Norway*
[2] *Norwegian Marine Technology Research Institute (MARINTEK), NO-7450 Trondheim, Norway*

Abstract: The flow around a circular cylinder in the vicinity of a rigid wall at Reynolds number 13100 is simulated using Large Eddy Simulations (LES) with Smagorinsky subgrid scale model. The main purpose of the present work is to investigate the flow behavior and the forces exerted on the cylinder near a rigid wall. The simulations with gap-to-diameter ratios (G/D) of 0.2, 0.6 and 1 are carried out in order to investigate the modifications of the flow field and vortex shedding due to the presence of the wall. Influence of the incoming boundary layer profile is investigated through two simulations with the logarithmic boundary layer inlet profile of thicknesses 0.48D and 1.6D and a simulation with a uniform inlet profile. The velocity field in the cylinder wake as well as the hydrodynamic values and the pressure distribution on the cylinder surface are used to understand the physics of the flow and to separate the influences of the wall proximity and the shear layers interaction. The results are compared to the experimental results obtained by Particle Image Velocimetry (PIV) and point-type pressure measurements.

Keywords: circular cylinder in the vicinity of a wall; Large Eddy Simulations; Smagorinsky model; gap-to-diameter ratio; boundary layer.

INTRODUCTION

Flow around a circular cylinder in the vicinity of a rigid wall is a topic of high interest in the marine technology environment. Free-spanning subsea pipelines, marine risers in the vicinity of the sea bed and circular elements of various bottom mounted marine structures are subjected to a continuous strain due to the exposure to current and waves. To improve the safety of such structures, it is important to understand the flow around and the forces exerted on them.

In order to do so, Large Eddy Simulations (LES) are utilized to simulate the fully three-dimensional (3D) flow around a circular cylinder in the vicinity of a rigid wall. For the flow around a circular cylinder in the unlimited fluid and a uniform inlet current, LES has proven to be a successful tool for modelling of such flow and capturing the three-dimensionality of the flow (Breuer (1998), Prsic et al. (2012)). A short overview of the numerical method is presented in the following section.

The simulations are made for the intermediate Reynolds number, Re = 13100 ($Re = U_\infty D/\upsilon$, where U_∞ is the free stream velocity, D is the cylinder diameter and υ is the kinematic viscosity of the fluid), corresponding to operational conditions of subsea pipelines. The mentioned Re is chosen partially due to the availability of detailed experimental measurements of the similar physical

problems. Particle Image Velocimetry (PIV) measurements were done by Price et al. (2002) for the Re range of 1200 to 4960, Alper Oner et al. (2008) for Re = 840, 4150, 9500, while Wang and Tan (2008) measured the flow features for Re very close to the one used in this study, Re = 1.4 * 10^4. Point measurements of the flow fields for the comparable Re are presented by Bearman and Zdravkovich (1978), Lei et al. (1999) and Han et al. (2009).

Several researchers have performed two-dimensional (2D) simulations using Reynolds – Averaged Navier – Stokes (RANS) equations. At a comparable Re, Brørs (1999) and Ong et al. (2010) performed calculations with RANS k-ε model and concluded upon the limitation of the 2D RANS models to predict the forces on the cylinder and the pressure distribution around it. At Re = 1440, Sarkar and Sarkar (2010) presented the results of the LES simulations which were in a good agreement with the experimental results of Price et al. (2002). Based on the mentioned research, LES is considered to be a promising tool for performing the simulations of the flow around a circular cylinder in the vicinity of the wall at an intermediate Re.

Several physical parameters are investigated: the influence of the gap-to-diameter ratio (G/D, where G is the distance between the cylinder and the wall), the influence of the boundary layer thickness (δ/D, where δ is the boundary layer thickness at the inlet) and the influence of the boundary layer profile.

NUMERICAL METHODS

Governing equations

In the present study, LES of the incompressible flow are performed. In order to simulate the flow, the incompressible Navier-Stokes equations need to be solved. In the filtered form, the continuity and the momentum equations can be written as:

$$\frac{\partial \bar{u}_i}{\partial x_i} = 0 \tag{1}$$

$$\frac{\partial \bar{u}_i}{\partial t} + \frac{\partial (\bar{u}_i \bar{u}_j)}{\partial x_j} = -\frac{1}{\rho}\frac{\partial \bar{p}}{\partial x_i} + \nu \frac{\partial^2 \bar{u}_i}{\partial x_j^2} - \frac{\partial \tau_{ij}}{\partial x_j} \tag{2}$$

where $\bar{u}_i$, i∈[1, 2, 3] denotes the filtered velocity component in streamwise (x), crossflow (y) and spanwise (z) direction respectively, x_i is assigned to the respective directions, ρ is the density of the fluid, $\bar{p}$ is the filtered pressure and τ_{ij} represents the non-resolvable subgrid stress, given by:

$$\tau_{ij} = \overline{u_i u_j} - \bar{u}_i \bar{u}_j \tag{3}$$

The commonly used subgrid scale model proposed by Smagorinsky (1963) is used to include the effect of subgrid scale motions, where the model coefficient C_s is kept constant. The studies of Breuer (1998, 2000) and Tremblay et al. (2002) have shown that the standard Smagorinsky model performs well in comparison to the more sophisticated subgrid scale models for a similar type of flow.

All the simulations are performed using the open source code OpenFOAM. The PISO algorithm (Pressure Implicit with Splitting of Operators) is used to solve the Navier-Stokes equations, described by Ferziger and Peric (2001). For the time integration, an implicit, backward differencing method of second order is used. Spatial schemes for the gradient terms are Gauss linear and Gauss limited linear. All of the above schemes are of second order accuracy.

Computational details

The LES simulations are performed on the rectangular computational domain with the streamwise length of 30D, extending from 10D in front of the cylinder to 20D in the wake, the crossflow height of (10.5+G)D extending from the rigid wall at G/D clearance to 10D above the cylinder center and the spanwise length of 4D. The domain dimensions are chosen from the previous experience with the simulations of the flow around a cylinder in free stream at Re = 13100 (Abrahamsen Prsic et al., 2013). Since the chosen domain is larger than the domains successfully used for the simulations of the flow with comparable Re presented by Liang and Cheng (2005) who used a 30D * 4D domain and Ong et al. (2012) using a 30D * 10D domain, it is believed that the domain boundaries do not influence the flow around the pipeline.

A body-fitted, structured O-mesh is divided in several zones, in order to maintain the control over the element size in the vicinity of the cylinder and at the bottom wall. Simulations with several mesh refinements are performed, see Table 1.

The boundary conditions are kept the same through the entire study. A boundary layer flow is specified by imposing a logarithmic profile at the inlet. Several boundary layer thicknesses are used, see Table 3. At the outlet, the pressure and the normal gradient of the velocity are set to zero. The top is defined as a symmetry plane, the side boundaries, perpendicular to the cylinder axis, have the periodic boundary condition imposed, while the no-slip condition is applied on the cylinder surface and the bottom wall.

TABLE 1: Numerical set-up for the case of cylinder close to the wall at G/D = 0.6 and δ/D = 1.6.

Case	G/D	δ/D	Computational domain (*D)	Total number of elements (million)	Number of elements circumferential	Δt (s)
g06_1	0.6	1.6	40*11.1*4	9.5	410	0.0001
g06_m1	0.6	1.6	40*11.1*4	7.5	360	0.0001
g06_m2	0.6	1.6	40*11.1*4	12.5	440	0.0001
g06_t1	0.6	1.6	40*11.1*4	9.5	410	0.00025
g06_t2	0.6	1.6	40*11.1*4	9.5	410	0.0005

CODE VALIDATION AND CONVERGENCE STUDIES

Cylinder in an infinite fluid at Re = 13100 – code validation

The code validation is performed for a simpler and more thoroughly investigated case – flow around a circular cylinder in an infinite fluid subjected to the uniform flow with the same Re = 13100, by comparison of the LES results to the available numerical and experimental results. Here, the domain extends over 8D in front, above and below the cylinder while the outlet is placed at 24D behind the cylinder. The spanwise domain length is again set to 4D. After performing the convergence study, the mesh of approximately 11 million elements and time-step of 0.0001s are used for the simulations (corresponding to case 13100_m3, Abrahamsen Prsic et al. (2013)).

The results are analysed through the time- and space-averaged standard hydrodynamic parameters of drag and lift coefficient. Mean drag coefficient of 1.31 and root-mean-square of lift coefficient of 0.54 show good agreement with the experimental results of Cantwell and Coles (1983) and numerical results of Breuer (2000) and Fang and Han (2011). The flow is further analysed through the velocity profiles in the cylinder wake. In Figure 1, the velocity field in the cylinder wake is presented through the time- and space-averaged streamwise velocity component (u) sampled in the (x, z) plane (Figure 1 a) and the (y, z) plane (Figure 1 b). In Figure 1 a, the velocity profile between x = 0.5D and x = 8D in the cylinder wake is compared to the DNS simulations of Tremblay et al. (2000), the LES simulations of Breuer (1998 b) for Re = 3900 and the experimental data of Cantwell and Coles (1983) for Re = 140000. It appears that qualitatively all the results show similar behaviour in the cylinder wake. According to the theory, an increase in Re leads to a shorter separation bubble. That causes the velocity minimum being located closer to the cylinder. This behaviour can be noticed on Figure 1 a, where the minimum velocity for the present results lies between the minima for the Re = 3900 and Re = 140000 simulations. Figure 1 b shows the streamwise velocity component sampled along the vertical cross sections located 1.01D behind the cylinder. Again, it appears that qualitatively the results are similar to the other numerical and experimental results. The present results agree better with the results for the Re = 3900 flow (Tremblay et al. (2000), Lourenco and Shih (1993)). That is in agreement with the theory of Zdravkovich (1990) which gathers the flows in the Re range 2000 to 20000 (and thus those with Re = 3900 and Re = 13100) in the flow class with the transition vortices in the free shear layers, while the Re = 140000 flow falls into the next flow class with fully turbulent shear layers.

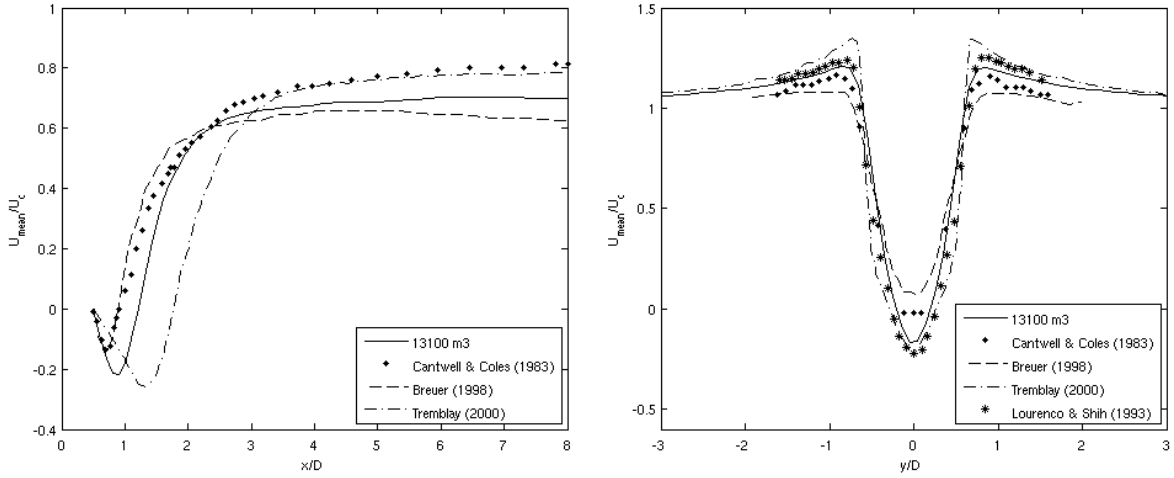

a) b)

Figure 1: Time- and space-averaged streamwise velocity component (u) profiles in the cylinder wake for a cylinder in an infinite fluid

a) in (x, z) plane, y = 0;

b) at x/D = 1.01 from the cylinder centre, in (y, z) plane

Symbols: - present study, • Re = 140000, Cantwell and Coles (1983), --- Re = 140000, Breuer (1998 b), -.- Re = 3900, Tremblay et al. (2000), * Re = 3900, Lourenco and Shih (1993).

Cylinder in the vicinity of a wall - convergence studies

The grid and time-step convergence studies are performed for the flow around a cylinder in the vicinity of a rigid wall at Re = 13100 for the case of G/D = 0.6 and δ/D = 1.6. The influence of the mesh and the time-step choice is analysed through the values of the time- and space-averaged drag coefficient ($\overline{C}_d$), the root-mean-square of the space averaged lift coefficient ($C_{l\,rms}$), Strouhal number (St), and the flow profiles in the cylinder wake. The aforementioned drag (C_d) and lift (C_l) coefficients are defined as: $C_d = F_d/(0.5\rho U_\infty^2 A)$ where F_d is the drag force obtained by integrating over the cylinder surface and A is the frontal area of the cylinder; $C_l = F_l/(0.5\rho U_\infty^2 A)$, where F_l is the integrated lift force. The Strouhal number is defined as $St = f\,D/U_\infty$, where f is the vortex shedding frequency. The time averaging is done for the fully developed flow.

In order to perform the grid convergence study, three different meshes are created, containing approximately 7.5 million elements (case g06 m1), 9.5 million (case g06 1) and 12.5 million elements (case g06 m2). The size of the elements at the cylinder and the wall surface is kept constant for these simulations. Details about the cases can be found in Table 1. Results presented in Figure 2 and Table 2, suggest that convergence is approached. The mesh refinement leads to a slight decrease in $\overline{C}_d$, but the difference in the $\overline{C}_d$ values does not exceed 1%. It is therefore concluded that the mesh with 9.5 million elements (case g06 1) provides a sufficient refinement.

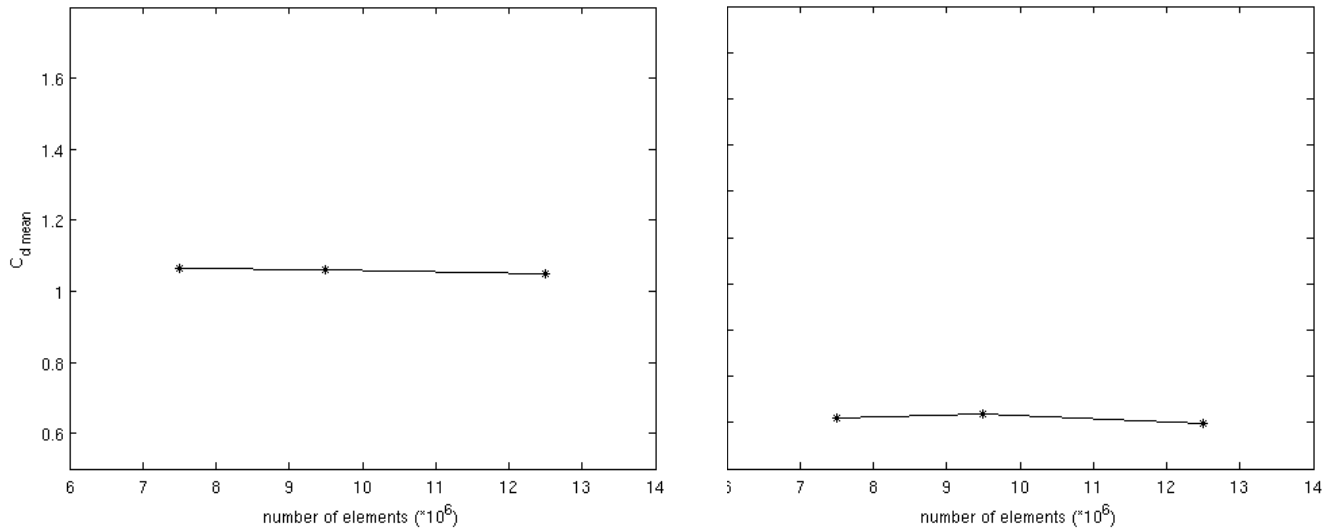

Figure 2: $\overline{C}_d$ and $C_{l\,rms}$ versus the number of elements in the mesh. Cases: g06_m1, g06_1, g06_m2 with G/D = 0.6 and δ/D = 1.6.

The influence of the numerical mesh is further investigated through the velocity profiles in the cylinder wake. The velocity field is sampled in the (x, z) plane, along several parallel cross-sections extending from the cylinder nape to 8D in the cylinder wake, distributed evenly along the cylinder span. Figure 3 shows the streamwise velocity component (u) averaged along the cylinder span. It can be noticed that the mesh refinement leads to a slightly less pronounced velocity minimum, located farther in the wake of the cylinder. The difference between the velocity minima in g06 m1 and g06 1 case is 27%, and it decreases to 12% for the comparison of cases g06 1 and g06 m2. It can also be noticed that the coarsest mesh (g06 m1) predicts higher velocities in the farther wake (x/D between 4 and 8) while

the two simulations with finer meshes show good agreement. Therefore it is concluded that, even though there is a small improvement from further mesh refinement, the mesh presented in g06 1 case can be considered sufficiently fine.

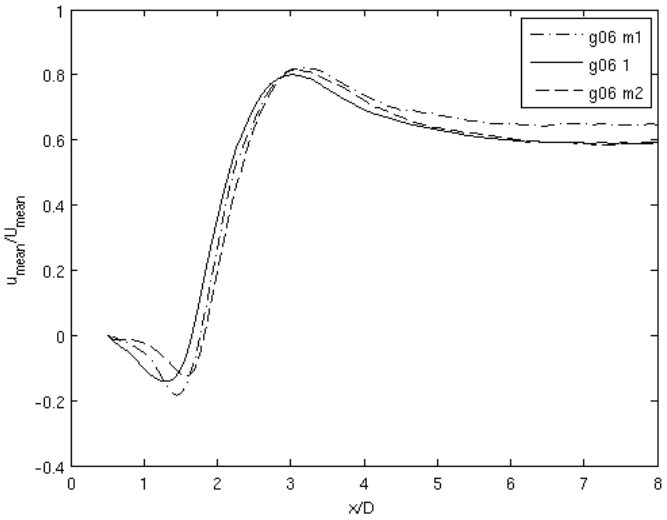

Figure 3: Time- and space-averaged streamwise velocity component (u) profile in the cylinder wake, in the (x, z) plane, y = 0 versus the number of elements in the mesh.

Similar analysis to the one of mesh convergence study is made for the time-step convergence. Time-steps of 0.0001 s, 0.00025 s and 0.00005 s are used in the simulations g06 1, g06 t1 and g06 t2 respectively. From Table 2, it can be concluded that the refinement of the time-step does not lead to significant changes in the integrated forces on the cylinder or St. $\overline{C}_d$ varies less than 5% between the smallest and the largest time-step. Figure 4 shows that the decrease in the time-step leads to a slightly longer wake with a less pronounced velocity minimum, but the differences are again very small. It is therefore concluded that the time-step of 0.0001s is sufficient for the further analysis.

TABLE 2: Mean flow parameter for the cylinder close to the wall at G/D = 0.6 and δ/D = 1.6.

Case	$\overline{C}_d$	$C_{l\,rms}$	St
g06_1	1.0611	0.1191	0.2912
g06_m1	1.0653	0.1093	0.2330
g06_m2	1.0486	0.0978	0.2912
g06_t1	1.101	0.1736	0.2330
g06_t2	1.1137	0.1947	0.2330

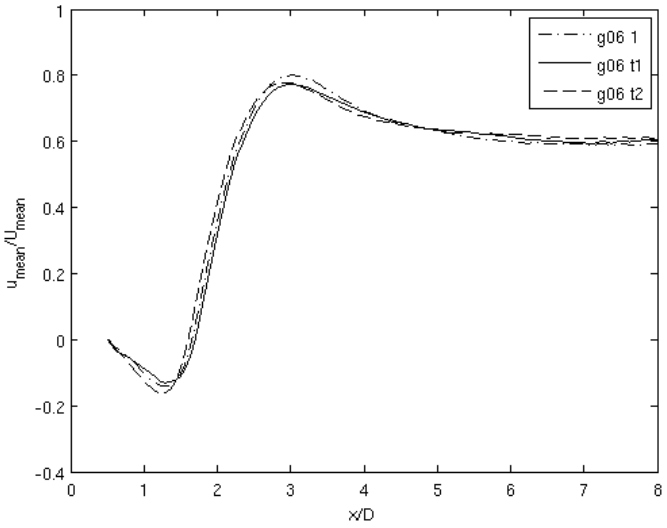

Figure 4: Time- and space-averaged streamwise velocity component (u) profile in the cylinder wake, in the (x, z) plane, y = 0 versus the time-step.

RESULTS: CYLINDER IN THE VICINITY OF A WALL AT Re = 13100

The main purpose of the present paper is to investigate the flow around a circular cylinder in the vicinity of a wall at Re = 13100. The influence of several physical parameters is of interest in this paper. The effect of G/D on the forces exerted on the cylinder and the properties of the flow in the wake is explored by choosing the gap values 0.2 (case g02 1), 0.6 (case g06 1) and 1 (case g1 1). The influence of δ/D is investigated by choosing the values δ/D = 0 (case g06 i1), 0.48 (case g06 i2) and 1.6 (case g06 1), where δ/D = 0 corresponds to a uniform inlet profile. In order to isolate the influence of G/D and δ/D, the domain size, the boundary conditions, the time-step and the over-all mesh characteristics as well as the element size on the cylinder and the wall are kept as close as possible to constant. Further details of the simulations are presented in Table 3.

TABLE 3: Numerical set-up for the case of cylinder close to the wall at various G/D and δ/D.

Case	G/D	δ/D	Computational domain (*D)	Total number of elements (million)	Number of elements circumferential	Δt (s)
g06_1	0.6	1.6	40*11.1*4	9.5	410	0.0001
g06_i1	0.6	0	40*11.1*4	9.5	410	0.0001
g06_i2	0.6	0.48	40*11.1*4	9.5	410	0.0001
g02_1	0.2	1.6	40*10.7*4	7.2	410	0.0001
g1_1	1	1.6	40*11.5*4	9.8	410	0.0001

Both experimental and numerical results show that $\overline{C}_d$ increases as G/D increases. Zdravkovich (2009) concludes that the influence of the wall proximity maintains its strong influence for small G/D ratios, but becomes insignificant as G/D exceeds 1, and thus the flow behaves similar to the case of a cylinder in infinite fluid. From Figure 5, presenting $\overline{C}_d$ and $C_{l\,rms}$ for various G/D, it is noticed that these features are captured in this study as elaborated in the following. The results (see Table 4) compare reasonably well to the experimental results of Lei et al. (1999) who measured $\overline{C}_d = 0.91$ for G/D = 0.2, $\overline{C}_d = 1.23$ at G/D = 0.6 and $\overline{C}_d = 1.37$ at G/D = 1. The differences in the results might be contributed to the fact that Lei et al. (1999) exposed the cylinder at G/D = 0.6 to the flow with δ/D = 0.48 while the present study is conducted with δ/D = 1.6. According to Zdravkovich (1985), the drag coefficient starts to decrease once the cylinder is immersed in the boundary layer. It is therefore to expect that the cylinder at G/D = 0.6 experiences a strong effect of the shear flow, while the cylinder at G/D = 1 is subjected to the smaller gradients of the shear flow and is thus less influenced by the boundary layer. Similar effect can be noticed on $C_{l\,rms}$ (Figure 5). According to Zdravkovich (2009), the vortex shedding is significantly suppressed for G/D < 0.3. It is therefore expected that the variations of the C_l and thus the mean value of $C_{l\,rms}$ are low for G/D = 0.2, which is also noticed in the present study. Due to almost suppressed vortex shedding, it is not possible to determine and discuss the Strouhal number. On the other hand, at G/D = 1, the flow is expected to behave similar to the flow around a cylinder in free stream. Such behaviour is manifested by a high $C_{l\,rms}$, comparable to the one presented in the validation study for the case of the cylinder in a free stream.

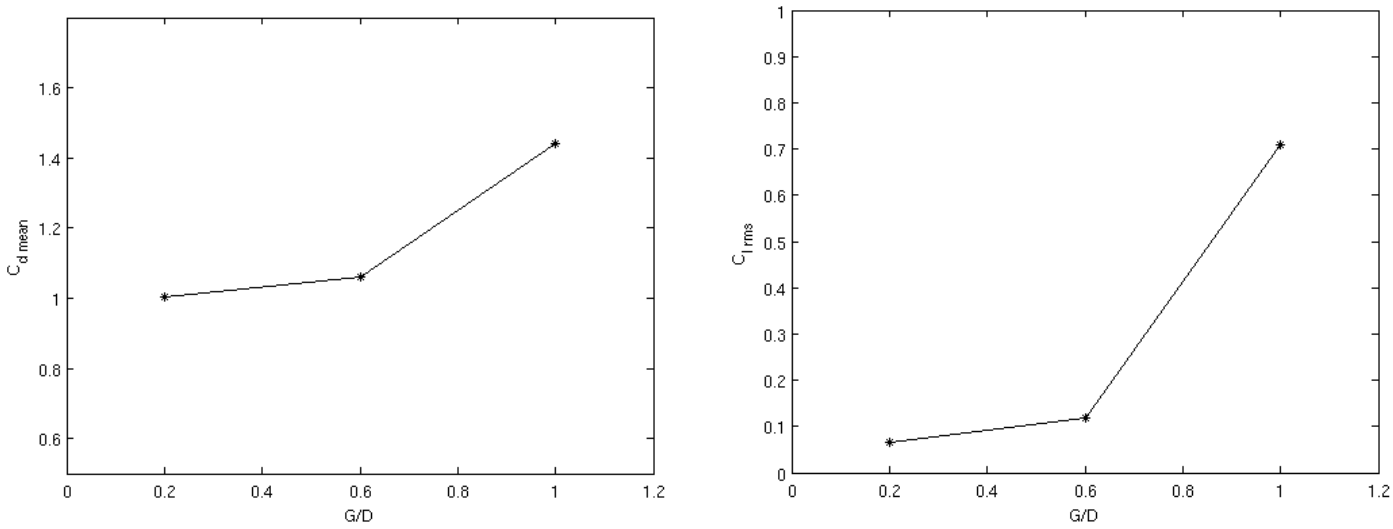

Figure 5: $\overline{C}_d$ and $C_{l\,rms}$ versus G/D for δ/D = 1.6.

The previous numerical research of Zhao et al. (2007) using a k-ω RANS model and Ong et al. (2010) using a k-ε RANS model show a significant under-prediction of the drag and lift coefficient, which generally is attributed to the two-dimensionality of the simulations. LES has therefore shown to be a good numerical tool for such 3D flow.

Further analysis of the physical behaviour of the flow can be made by analysing the velocity profiles in the cylinder wake. The velocity field is sampled in the (y, z) plane, along parallel cross-sections located at several distances distributed from the cylinder centreline (x/D = 0) to x/D = 8.5D in the cylinder wake. The time-averaged velocity profiles are presented in Figure 6. In the vicinity of the cylinder, a slight increase in the velocities can be noticed for all the G/D. Observing the velocity

profiles at x/D = 1.5 and further in the wake, a sudden velocity decrease is noticed for the cylinder very near to the wall, while an increase in G/D allows the higher velocities in the vicinity of the wall in the cylinder wake.

TABLE 4: Mean flow parameter for the cylinder close to the wall at at various G/D and δ/D.

Case	$\overline{C}_d$	$C_{l\,rms}$	St
g06_1	1.0611	0.1191	0.2912
g06_i1	1.4374	0.6141	0.2330
g06_i2	1.1608	0.1628	0.2912
g02_1	1.0053	0.0666	0
g1_1	1.4406	0.7100	0.2330

A similar behaviour is mentioned by Han et al. (2009) who measured the velocities behind the cylinder at G/D = 0.3, 0.5 and 1 for Re in the range from 1.67 $*10^4$ to 4.37 * 10^4. Sarkar and Sarkar (2009) also noticed that the flow with G/D = 0.25 yields a fairly large velocity deficit in the region between 2D and 3D behind the cylinder. They attributed this to the strong coupling between the inner-shear layer and the boundary layer. Alper Oner et al. (2008) described the disturbed velocity field in the wake of the cylinder at G/D = 1 as nearly symmetrical around its horizontal axis. The same observation is made from Figure 6, leading to the conclusion that the influence of the wall looses its significance as G/D increases towards 1.

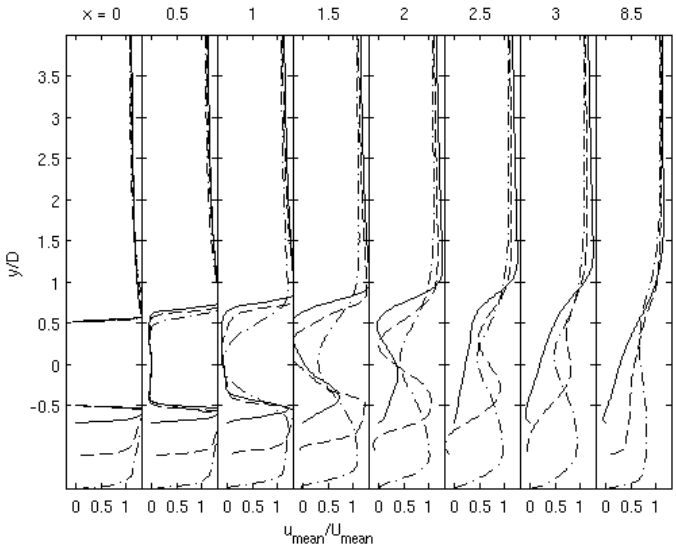

Figure 6: Time-averaged streamwise velocity component (u) profile in the cylinder wake, in the (y, z) plane, x/D = 0, 0.5, 1, 1.5, 2, 2.5, 3, 8.5. Symbols: — G/D = 0.2, - - G/D = 0.6, -·- G/D = 1.

As mentioned briefly before, the behaviour of the flow around a cylinder in the vicinity of the wall depends not only on G/D, but aso on the shape of the incoming boundary layer profile. Therefore three simulations with constant G/D = 0.6 and changing thickness of the inlet boundary layer are performed. The details are presented in Table 3. The logarithmic profile is chosen to simulate a naturally developed boundary layer profile near a flat, rigid bed. The flow is allowed to develop over 10D before it reaches the cylinder.

Contrary to the extensive number of studies investigating the influence of G/D, the data available on the influence of δ/D are scarce. Zdravkovich (1985) conducted a series of experiments for a higher Re varying between $4.8 * 10^4$ and $1.4 * 10^5$, which is in the same flow-class as the present study, and is therefore considered to behave qualitatively similar. He concluded that the drag coefficient starts to decrease once the cylinder is immersed in the boundary layer. He therefore continued to analyse the ratio of gap and boundary layer thickness, G/δ, noticing that $\overline{C}_d$ decreases as G/δ decreases below 1 and maintains a slowly increasing trend for G/δ > 1. For $Re = 6.1 * 10^4$, he obtained $\overline{C}_d = 1.05$, 0.96 and 0.64 for G/δ = 0.4, 1.2 and 2, respectively. The same trend is observed in the present study, resulting in $\overline{C}_d = 1.43$ for g06 i1 case (δ/D → 0, G/δ → ∞), $\overline{C}_d = 1.16$ for g06 i2 case (δ/D = 0.48, G/δ = 1.25) and $\overline{C}_d = 1.06$ for g06 1 case (δ/D =1.6, G/δ = 0.375); see Figure 7. Zdravkovich (1985) noticed a similar behaviour for the $C_{l\,rms}$ showing a sudden decrease for the cylinder immersed in the boundary layer. That trend is also noticed here, presented in Figure 7.

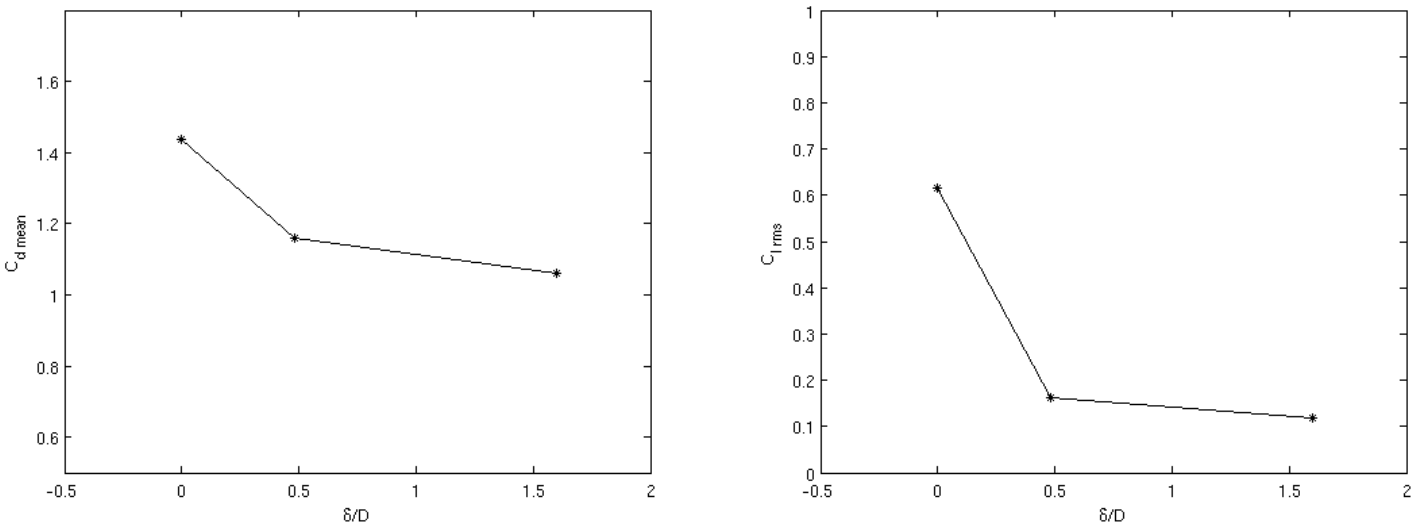

Figure 7: $\overline{C}_d$ and $C_{l\,rms}$ versus δ/D for G/D = 0.6.

For a more detailed understanding of the δ/D influence, the mean pressure coefficient distribution is analysed. The mean pressure coefficient (C_p) is defined as the time-average for the fully developed flow of the instantaneous pressure coefficient $C_{p\,in} = (p'-p_\infty)/(0.5\rho U_\infty^2)$ where p' is the instantaneous pressure at the sampling point and p_∞ is the pressure in the undisturbed flow. Figure 8 shows the C_p distributions around the cylinder, where θ = 0 corresponds to the point at the cylinder closest to the wall and θ increases in the clockwise direction. It can be noticed that a thicker boundary layer leads to a less pronounced maximum in C_p and a less negative base pressure. The difference is most pronounced between the case where the cylinder is completely out of the boundary layer and the two cases of the cylinder partially and fully immersed in the boundary layer shear flow. This behaviour is also noticed in the experimental study of Lei et al. (1999) and the simulations by Ong et al. (2012). Lei et al. (1999) suggest that the physical influence of the shear flow on the pressure distribution can also be connected to the displacement of the separation points. This behaviour needs further investigations.

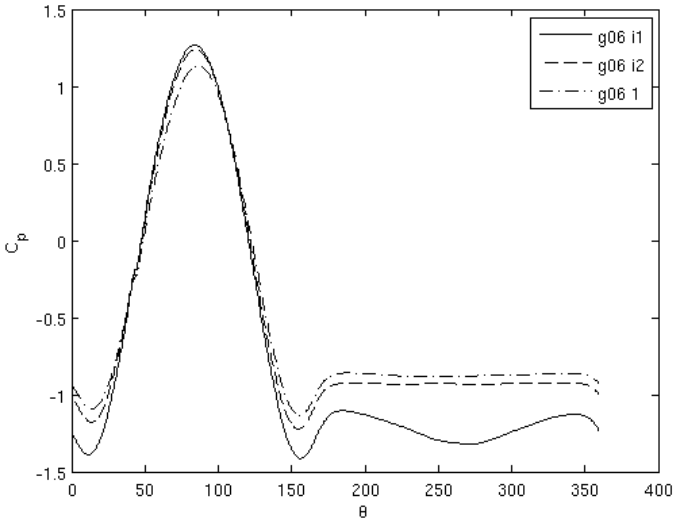

Figure 8: C_p distribution versus δ/D ratio for G/D = 0.6.

CONCLUSIONS

Near-bed flow influences on the circular subsea pipeline in the vicinity of the sea-bed at Re = 13100 are investigated. LES simulations with a Smagorinsky sub-grid scale model are performed. The influences of the clearance between the cylinder and the bed as well as of the boundary layer thickness on the forces exerted on the cylinder, and the flow field in the cylinder wake, are presented. The main conclusions are:

1) Comparison of the present results with the experimental results and 2D RANS numerical models leads to a conclusion that LES offers a good numerical tool for the chosen type of flow.
2) G/D has a strong influence on the forces on the cylinder and the development of the flow in the wake. For G/D smaller than the critical gap, the vortex shedding is suppressed. Such behaviour is noticed in the present study for G/D = 0.2. Increasing G/D, the vortex shedding develops (presented for G/D = 0.6). Due to the reduced interaction of the bottom and the cylinder boundary layer for even larger G/D, the flow approaches the behaviour of the cylinder in an infinite fluid and uniform velocity field.
3) Although the vicinity of the wall has a significant influence on the general flow characteristics, it is observed that the flow depends on the thickness of the boundary layer. Even for a relatively small G/D = 0.6, the flow around the cylinder, which is not immersed in the boundary layer, resembles the cylinder in an infinite fluid. For larger δ/D where the cylinder is subjected to the shear flow, the influence of the boundary layer gives lower $\overline{C}_d$ and $C_{l\,rms}$ as well as changes in the C_p distribution around the cylinder.

References

Abrahamsen Prsic, M., Ong, M. C., Pettersen, B., Myrhaug D., 2013. Large-eddy simulations of three dimensional flow around a smooth circular cylinder in a uniform current in the subcritical flow regime. Under review for Ocean Engineering.

Alper Oner, A., Salih Kirgoz, M., Sami Akoz, M., 2008. Interaction of a current with a circular cylinder near a rigid bed. Ocean Engineering, 35, 1492-1504.

Bearman, P. W., Zdravkovich, M. M., 1978. Flow around a circular cylinder near a plane boundary. Journal of Fluid Mechanics, 89, 33-47.

Breuer, M., 1998. Large eddy simulation of the subcritical flow past a circular cylinder: numerical and modeling aspects. International Journal for Numerical Methods in Fluids, 28, 1280-1302.

Breuer, M., 2000. A challenging case for large eddy simulation of high Reynolds number circular cylinder flow. International Journal of Heat and Fluid Flow, 21, 648-654.

Brørs, B., 1999. Numerical modelling of flow and scour at pipelines. Journal of Hydraulic Engineering, Vol 125, No. 5, 511-523.

Cantwell, B., Coles, D., 1983. An experimental study of entrainment and transport in the turbulent near wake of a circular cylinder. Journal of Fluid Mechanics, 136, 321-374.

Fang, Y., Han, Z., 2011. Numerical experimental research on the hydrodynamic performance of flow around a three dimensional circular cylinder. Applied Mechanics and Materials, 90-93, 2778-2781.

Ferziger, J. H., Peric, M., 2001. Computational methods for fluid dynamics. 3rd Ed, Springer-Verlag, Berlin, Germany.

Han, Y., Shi, B., Ren, X., Jing, X., 2009. Experimental study on the distribution of velocity and pressure near a submarine pipeline. J. Ocean Univ. China (Oceanic and Coastal Sea Research), 8(4), 404-408.

Lei, C., Cheng, L., Kavanagh, K., 1999. Re-examination of the effect of a plane boundary on force and vortex shedding of a circular cylinder. Journal of Wind Engineering and Industrial Aerodynamics, 80, 263-286.

Liang, D., Cheng, L., 2005. Numerical modeling of flow and scour below a pipeline in currents; Part 1. Flow simulation. Coastal Engineering, 52, 25-42.

Lourenco, L. M., Shih, C., 1993. Characteristics of the plane turbulent near wake of a circular cylinder, a particle image velocimetry study. Published in Beaudan, P., Moin, P., 1994. Numerical experiments on the flow past a circular cylinder at sub-critical Reynolds number. Report no. TF-62, Thermosciences Division, Department of Mechanical Engineering, Stanford University.

Ong, M. C. ,Utnes, T., Holmedal, L. E., Myrhaug, D., Pettersen, B., 2010. Numerical simulation of flow around a circular cylinder close to a flat seabed at high Reynolds numbers using a k- ε model. Coastal Engineering, v 57, n 10, p 931-947.

Ong, M. C. ,Utnes, T., Holmedal, L. E., Myrhaug, D., Pettersen, B., 2012. Near-bed flow mechanisms around a circular marine pipeline close to a flat seabed in the subcritical flow regime using a k - ε model. Journal of Offshore Mechanics and Arctic Engineering, v 134, n 2, p 021803.

Price, S. J., Sumner, D., Smith, J. G., Leong., K., Paidoussis, M. P., 2002. Flow visualization around a circular cylinder near to a plane wall. Journal of Fluids and Structures, 16(2), 175-191.

Prsic, M., Ong M. C., Pettersen, B., Myrhaug, D., 2012. Large eddy simulations of three-dimensional flow around a pipeline in a uniform current. Proceedings of the 31st International Conference on Offshore Mechanics and Arctic Engineering, Rio De Janeiro, Brazil, OMAE2012-83144.

Sarkar, S., Sarkar, S., 2010. Vortex dynamics of a cylinder wake in proximity to a wall. Journal of Fluids and Structures, 26, 19-40.

Smagorinsky, J., 1963. General circulation experiments with the primitive equations. Monthly Weather Review, 91-3, 99-164.

Tremblay, F., Manhart, M., Friedrich, R., 2000. DNS of flow around the circular cylinder at subcritical Reynolds number with Cartesian grids. Proceedings of the 8th European Turbulence Conference, EUROMECH, Barcelona, Spain, 659-662.

Wang, X. K., Tan, S. K., 2008. Comparison of flow patterns in the near wake of a circular cylinder and a square cylinder placed near a plane wall. Ocean Engineering, 35 458-472.

Zdravkovich, M. M., 1985. Forces on a circular cylinder near a plane wall. Applied Ocean Research, Vol 7, No. 4, 197-201.

Zdravkovich, M. M., 1990. Conceptual overview of laminar and turbulent flows past smooth and rough circular

cylinders. Journal of Wind Engineering and Industrial Aerodynamics, 33, 53-62.

Zdravkovich , M. M., 2009. Flow around circular cylinders. Vol.2: Applications. Oxford University Press, Oxford, United Kingdom.

Zhao, M., Cheng, L., Teng, B., 2007. Numerical modeling of flow and hydrodynamic forces around a piggyback pipeline near the seabed. Journal of Waterway, Port, Coastal and Ocean Engineering, v 133, n 4, p 286-295.